

Fabrication of TiO₂ and Cytochrome *c* Alternate Ultrathin Films via a Gas-phase Surface Sol–Gel Process

Do-Hyeon Yang,¹ Naoki Takahara,¹ Naoki Mizutani,¹ Seung-Woo Lee,^{*1} and Toyoki Kunitake^{1,2}

¹Graduate School of Environmental Engineering, the University of Kitakyushu, 1-1 Hibikino, Kitakyushu 808-0135

²Frontier Research System (FRS), The Institute of Physical and Chemical Research (RIKEN), 2-1 Hirosawa, Wako 351-0198

(Received May 12, 2006; CL-060565; E-mail: leesw@env.kitakyu-u.ac.jp)

A gas-phase surface sol–gel process was developed for facile preparation of ultrathin TiO₂ gel/Cyt. *c* multilayered films. Positively charged Cyt. *c* protein was alternately assembled with TiO₂ gel layer that was prepared by deposition of Ti(O^{*n*}-Bu)₄ vapor and subsequent hydrolysis. The adsorbed Cyt. *c* molecule was covered with a 0.7-nm thick layer of TiO₂ gel and the protein characteristics were preserved without denaturation in the multilayered film.

Nano-structured metal oxide thin films are known to display advantages for designing unique chemical functions like specific adsorption of organic molecules, improved catalytic properties and the capture of light energy. The sol–gel method is one of the most important techniques for the preparation of ultrathin films of metal oxides and metal oxide/organic hybrid materials.¹ During the last decade, dry approaches such as chemical vapor deposition (CVD), molecular beam epitaxy (MBE), and atomic layer deposition (ALD) have attracted considerable attention as methods for fabricating high quality (defect-free) ultrathin films of metal oxides.² On the other hand, the surface sol–gel process³ has been extensively studied as a corresponding wet process. This process is based on adsorption of metal alkoxide molecules from solution onto hydroxylated surfaces and subsequent hydrolysis to give nanometer-thick oxide films. Unfortunately, biological applications of these conventional sol–gel processes, both dry and wet, are limited, because of their processing conditions such as high vacuum, high temperature, and the use of organic solvents that will induce denaturation of biomolecules.

Recently, effective immobilization of native proteins in metal oxide matrices has been reported. Kimizuka et al. utilized a liquid-phase deposition (LPD) process that enables preparation of anatase TiO₂ by boric acid-promoted hydrolysis of titanium hexafluoride in water.⁴ This process was proposed as a means to prevent denaturation of cytochrome *c* (Cyt. *c*). Ju and co-workers reported a vapor-deposition sol–gel process,⁵ where titanium isopropoxide vapor was introduced into a thin layer of aqueous horseradish peroxidase (HRP), forming a TiO₂/HRP film. This vapor process is valuable from the viewpoint of not using organic solvents, but it has some drawbacks in practical applications: (1) the sol–gel reaction is very slow, since the concentration of metal alkoxides in the gas phase is relatively low compared with that in solution, and (2) the size and shape of substrates are restricted.

In this study, we describe a novel approach to overcome drawbacks of the conventional sol–gel methods in the case of the biological application. An important feature of this approach is that ultrathin metal oxide films of controlled thickness can be fabricated from metal alkoxides in gas phase. Upon adsorption

of the metal alkoxide vapor, the surface sol–gel procedures can be operated. We name this process a “gas-phase surface sol–gel (GSSG) process.” Figure 1a shows a schematic illustration of this process for a TiO₂ gel/Cyt. *c* ultrathin multilayer.

A gold-coated quartz crystal microbalance (QCM) resonator (9 MHz, USI System, Fukuoka) was hydroxylated by 2-mercaptoethanol as described previously.³ Titanium *n*-butoxide, Ti(O^{*n*}-Bu)₄, was heated in a sealed bottle at 85 °C, and the vaporized Ti(O^{*n*}-Bu)₄ was carried with nitrogen gas at a flow rate of 3 L/min. It was allowed to deposit on the gold-coated QCM electrode for 5 min, and the physisorbed alkoxide was removed by flushing nitrogen gas. Then, the QCM electrode was immersed in deionized water for 1 min, dried with nitrogen gas, and the frequency was measured. Subsequently, the TiO₂ gel-deposited electrode was immersed in a phosphate buffer solution of Cyt. *c* (1 mg/mL, pH 7.0) for 10 min at 25 °C and rinsed with deionized water, and the frequency was measured after drying with nitrogen gas. This alternate deposition of TiO₂ gel and Cyt. *c* layers was repeated 10 times.

Figure 1b shows QCM frequency changes due to the alternate adsorption. The QCM frequency linearly decreases with adsorption cycles, indicating regular growth of the TiO₂ gel/

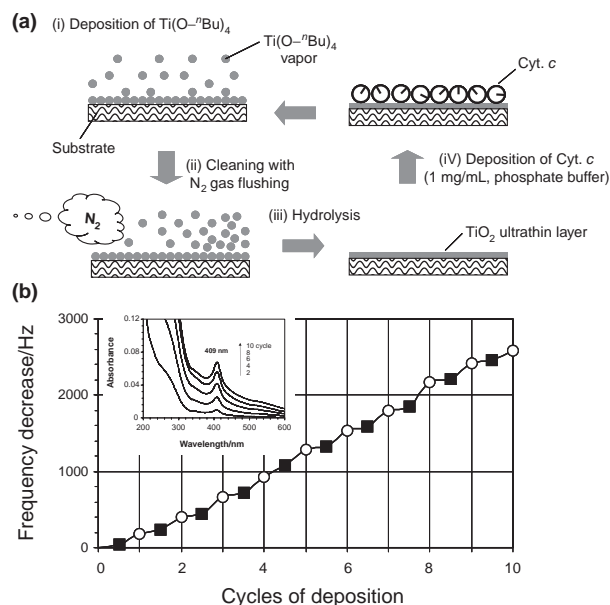


Figure 1. Schematic illustration of deposition of TiO₂ gel and Cyt. *c* via a gas-phase surface sol–gel (GSSG) process (a), and QCM frequency shifts (b). Ti(O^{*n*}-Bu)₄ vapor with nitrogen gas carrier (3 L/min) (■); Cyt. *c*, 1 mg/mL (pH 7, 25 °C) (○). The inset of Figure 1b shows UV–vis spectral changes due to alternate adsorption of Ti(O^{*n*}-Bu)₄ and Cyt. *c*.

Cyt. *c* multilayer film. Average frequency changes for the adsorption of $\text{Ti}(\text{O}-^n\text{Bu})_4$ and Cyt. *c* are 47 ± 9 and 191 ± 35 Hz, respectively. The thickness of each layer can be estimated by using Sauerbrey's equation.⁶ The ΔF value of 47 Hz corresponds to a thickness increase by ca. 0.7 nm for the TiO_2 gel layer, using the density of bulk TiO_2 gel (1.7 g/cm^3).³ Similarly, the thickness of the adsorbed Cyt. *c* layer is estimated to be 4.0 nm, assuming a density of the protein layer to be 1.3 g/cm^3 .⁷ The adsorption density of Cyt. *c* can be calculated as 0.26 proteins/ nm^2 from the frequency change ($\Delta F = 191 \text{ Hz}$) of the QCM electrode with an area of 0.32 cm^2 for both sides and the Cyt. *c* molecular weight (MW 12384). This figure is ca. 2 times as large as the density of a protein monolayer ($0.128 \text{ proteins/nm}^2$) that is theoretically calculated by considering Cyt. *c* ($2.5 \times 2.5 \times 3.7 \text{ nm}^3$) as a spherical particle with a diameter of ca. 3.0 nm .⁸

The inset of Figure 1b shows UV-vis absorption spectra of the alternate multilayer on a quartz substrate. The absorbance at the Soret band increased in proportion to the adsorption cycle up to 10 cycles, together with the increased absorbance of TiO_2 gel in the near UV and visible region. The peak of the Soret band is located at the same wavelength as that of native Cyt. *c* in phosphate buffer (pH 7). This suggests that the steric structure of Cyt. *c* is preserved in the film. The amount of immobilized Cyt. *c* molecules during one adsorption cycle was estimated from the absorbance increase per cycle and the molar extinction coefficient at 409 nm ($\epsilon = 96 \text{ mM}^{-1} \text{ cm}^{-1}$).⁹ The adsorption density of Cyt. *c* on one side of the quartz plate was estimated to be $0.23 \text{ proteins/nm}^2$ from the average absorbance difference ($\Delta \text{Abs} = 0.0073$, $n = 10$) before and after Cyt. *c* adsorption. This value is 1.8 times larger than the theoretical protein coverage of Cyt. *c* ($0.128 \text{ proteins/nm}^2$) and is consistent with that estimated from the QCM data ($0.26 \text{ proteins/nm}^2$).

These results indicate that Cyt. *c* is adsorbed nearly as a bilayer on the surface of a TiO_2 gel layer. It is important to know whether the surface is uniformly covered by Cyt. *c* molecules. Therefore, the morphology of TiO_2 gel/Cyt. *c* multilayers was investigated by using atomic force microscopy (AFM). Figures 2a, 2b, and 2c are AFM images of the $(\text{TiO}_2 \text{ gel})_{20}$, $(\text{TiO}_2 \text{ gel})_{20}/\text{Cyt. } c$, and $(\text{TiO}_2 \text{ gel}/\text{Cyt. } c)_{10}$ multilayered films on quartz substrates, respectively. The surface of the TiO_2 gel film itself is extremely smooth with its root-mean-square (RMS) roughness of 0.52 nm, though scars of the quartz substrate are observed in some areas (Figure 2a). This RMS roughness increased to 1.32 nm by the adsorption of Cyt. *c* and the surface was densely covered with the adsorbed Cyt. *c* molecules (Figure 2b). Such surface morphology is also observed in the multilayered film of $(\text{TiO}_2 \text{ gel}/\text{Cyt. } c)_{10}$. The surface is composed of independently dispersed, close-packed Cyt. *c* molecules, and the RMS roughness remained to be 1.93 nm (Figures 2c). It is clear that Cyt. *c* is immobilized nearly as a bilayer between TiO_2 gel ultrathin layers.

In conclusion, we examined a gas-phase surface sol-gel process for facile preparation of ultrathin TiO_2 gel/Cyt. *c* multilayered films. Close-packed Cyt. *c* proteins are assembled nearly as a bilayer without denaturation by alternation of TiO_2 gel layer. This process has several advantages compared with previous wet processes. First, we can avoid direct contact of proteins with organic solvents, so that denaturation would not occur. Secondly, this process is less time-consuming and milder compared

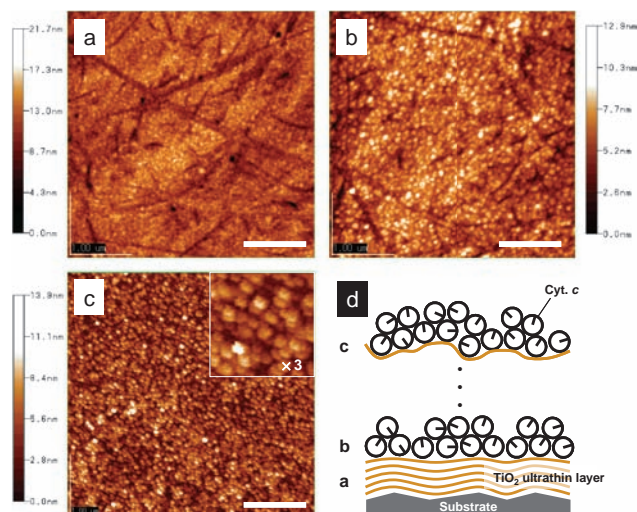


Figure 2. AFM images of $(\text{TiO}_2 \text{ gel})_{20}$ film (a), $(\text{TiO}_2 \text{ gel})_{20}/\text{Cyt. } c$ film (b), and $(\text{TiO}_2 \text{ gel}/\text{Cyt. } c)_{10}$ film (c). Schematic illustration of TiO_2 gel/Cyt. *c* alternate adsorption (d). AFM measurements were carried out by noncontact mode on a Scanning Probe Microscope JSPM-5200 (JEOL). Scale bar represents $1 \mu\text{m}$.

with the conventional vapor-deposition and LPD processes. Although we still need to confirm full conservation of the biological function in the ultrathin TiO_2 gel matrix, this new technique should be effective for the preparation of a variety of metal oxide/native protein hybrid layers.

This work was supported by the MEXT via the Kitakyushu Knowledge-based Cluster Project and a Grant-in-Aid for Science Research (No. 17651075) from the Ministry of Education, Culture, Sports, Science and Technology of Japan.

References and Notes

- 1 *Sol-gel Science: The Physics and Chemistry of Sol-gel Processing*, ed. by C. J. Brinker, G. W. Scherer, Academic Press, San Diego, **1990**; C. Sanchez, F. Ribot, *New J. Chem.* **1994**, *18*, 1007; A. Sellinger, P. M. Weiss, A. Nguyen, Y. Lu, R. A. Assink, W. Gong, C. Jeffrey Brinker, *Nature* **1998**, *394*, 256.
- 2 H. Kumagai, M. Matsumoto, K. Toyoda, M. Obara, M. Suzuki, *Thin Solid Films* **1995**, *263*, 47; H. Toda, *Langmuir* **1995**, *11*, 3281; M. A. Cameron, I. P. Gartland, J. A. Smith, S. F. Diaz, S. M. George, *Langmuir* **2000**, *16*, 7435.
- 3 I. Ichinose, H. Senzu, T. Kunitake, *Chem. Lett.* **1996**, 831; I. Ichinose, T. Kawakami, T. Kunitake, *Adv. Mater.* **1998**, *10*, 535; S.-W. Lee, I. Ichinose, T. Kunitake, *Langmuir* **1998**, *14*, 2857.
- 4 N. Kimizuka, M. Tanaka, T. Kunitake, *Chem. Lett.* **1999**, 1333.
- 5 J. Yu, H. Ju, *Anal. Chem.* **2002**, *74*, 3579; J. Yu, S. Liu, H. Ju, *Biosens. Bioelectron.* **2003**, *19*, 509.
- 6 G. Sauerbrey, *Z. Phys.* **1959**, *155*, 206.
- 7 Y. Lvov, K. Ariga, I. Ichinose, T. Kunitake, *J. Am. Chem. Soc.* **1995**, *117*, 6117.
- 8 I. Ichinose, R. Takaki, K. Kuroiwa, T. Kunitake, *Langmuir* **2003**, *19*, 3883. The mass increase expected from the theoretical protein coverage is estimated to cause a frequency decrease of 94 Hz.
- 9 L. L. Wood, S.-S. Cheng, P. L. Edmiston, S. S. Saavedra, *J. Am. Chem. Soc.* **1997**, *119*, 571.